Stimulation-induced changes in NADH fluorescence and mitochondrial membrane potential in lizard motor nerve terminals

Janet Talbot, John N. Barrett, Ellen F. Barrett and Gavriel David

Department of Physiology and Biophysics, Miller School of Medicine, University of Miami, PO Box 016430, Miami, FL 33101, USA

To investigate mitochondrial responses to repetitive stimulation, we measured changes in NADH fluorescence and mitochondrial membrane potential (Ψ_m) produced by trains of action potentials (50 Hz for 10–50 s) delivered to motor nerve terminals innervating external intercostal muscles. Stimulation produced a rapid decrease in NADH fluorescence and partial depolarization of Ψ_m. These changes were blocked when Ca^{2+} was removed from the bath or when N-type Ca^{2+} channels were inhibited with ω-conotoxin GVIA, but were not blocked when bath Ca^{2+} was replaced by Sr^{2+}, or when vesicular release was inhibited with botulinum toxin A. When stimulation stopped, NADH fluorescence and Ψ_m returned to baseline values much faster than mitochondrial $[Ca^{2+}]$. In contrast to findings in other tissues, there was usually little or no poststimulation overshoot of NADH fluorescence. These findings suggest that the major change in motor terminal mitochondrial function brought about by repetitive stimulation is a rapid acceleration of electron transport chain (ETC) activity due to the Ψ_m depolarization produced by mitochondrial Ca^{2+} (or Sr^{2+}) influx. After partial inhibition of complex I of the ETC with amytal, stimulation produced greater Ψ_m depolarization and a greater elevation of cytosolic $[Ca^{2+}]$. These results suggest that the ability to accelerate ETC activity is important for normal mitochondrial sequestration of stimulation-induced Ca^{2+} loads.

(Resubmitted 11 December 2006; accepted 26 December 2006; first published online 4 January 2007)
Corresponding author G. David: Department of Physiology and Biophysics, Miller School of Medicine, University of Miami, PO Box 016430, Miami, FL 33101, USA. Email: gdavid@med.miami.edu

Stimulation with high-frequency trains of action potentials imposes multiple potential energy demands on motor nerve terminals, including those associated with mobilization and recycling of synaptic vesicles, and with extrusion of Na^+ and Ca^{2+} across the plasma membrane. In these terminals, large Ca^{2+} loads are temporarily sequestered in the mitochondrial matrix (David *et al.* 1998; David, 1999; Suzuki *et al.* 2002). This sequestration also represents an energy demand, because entry of Ca^{2+} via the mitochondrial uniporter/channel (Kirichok *et al.* 2004) dissipates some of the potential gradient (Ψ_m, normal value -150 to -200 mV) generated across the inner mitochondrial membrane by H^+ extrusion via complexes I, III and IV of the electron transport chain (ETC, reviewed by Gunter & Pfeiffer, 1990).

Changes in mitochondrial metabolic functions evoked by various forms of stimulation (electrical, high $[K^+]$ and glutamatergic agonists) have been assessed by measuring changes in NADH fluorescence and Ψ_m in many regions of the nervous system (Rodriguez-Estrada, 1975; Mironov & Richter, 2001; Schuchmann *et al.* 2001; Shuttleworth *et al.* 2003; Kann *et al.* 2003; Kasischke *et al.* 2004; Kosterin *et al.* 2005), as well as the somata of individual dorsal root ganglion and Purkinje neurons (Duchen, 1992; Hayakawa *et al.* 2005) and chromaffin cells (Warashina, 2006). Most of these studies report a small, transient reduction in NADH fluorescence accompanied by Ψ_m depolarization, followed by a much larger, prolonged increase in NADH fluorescence. Similar stimulation-induced changes in NADH fluorescence and Ψ_m have also been reported in non-neuronal tissues (Pralong *et al.* 1994; Hajnoczky *et al.* 1995; Rohacs *et al.* 1997; Robb-Gaspers *et al.* 1998; Voronina *et al.* 2002; Brandes & Bers, 2002; Luciani *et al.* 2006). In many cases, these stimulation-induced changes in NADH fluorescence and Ψ_m were wholly or partially dependent on bath $[Ca^{2+}]$. Because NADH carries reducing equivalents from the tricarboxylic acid (TCA) cycle to complex I of the ETC, decreases in NADH fluorescence have been attributed to acceleration of ETC activity caused by Ψ_m depolarization. Increases in NADH fluorescence have been attributed to increased activity of the TCA cycle, due, for example, to stimulation

 DOI: 10.1113/jphysiol.2006.126383

by increased matrix [Ca^{2+}] of certain dehydrogenases (pyruvate, NAD^+-isocitrate and 2-oxoglutarate; reviewed by McCormack *et al.* 1990).

In metabolic measurements from CNS slices, components arising from presynaptic terminals are mixed with components arising from neuronal somata and axons as well as non-neuronal cells. To obtain a clearer picture of presynaptic changes, we measured stimulation-induced changes in NADH fluorescence and Ψ_m in individual motor nerve terminals. The dominant change in NADH fluorescence was a rapid decrease that persisted throughout stimulation and was independent of transmitter release. Evidence suggests that this decrease reflected acceleration of ETC activity due to the Ψ_m depolarization produced by influx of Ca^{2+} into mitochondria. Surprisingly, the prolonged poststimulation increase in NADH fluorescence so prominent in other tissues was small or absent.

Methods

Preparation, solutions and stimulation

Neuromuscular preparations from external intercostal muscles were dissected from the lizard *Anolis sagrei*. Animals were decapitated and pithed after they had been killed by exposure to 100% CO_2, using protocols approved by the University of Miami Animal Care and Use Committee. The preparation was mounted in a silicon chamber constructed on a no. 1 glass coverslip and bathed in normal lizard saline (NLS) composed of (mM): NaCl 157, KCl 4, $CaCl_2$ 2, $MgCl_2$ 2, glucose 5.5 and Hepes 1; pH 7.4. Each preparation included multiple intercostal muscle segments ($n = 4$–6), each innervated by its own motor nerve. All experiments were performed at room temperature (23-25°C), within the physiological range for lizards.

In the experiment of Fig. 6, complex I of the ETC was inhibited using 5 mM amytal. We used amytal instead of the more commonly used complex I inhibitor rotenone because the effects of amytal were easier to titrate to achieve the desired partial block (for review of the effects of amytal and rotenone see Degli-Esposti, 1998). In the presence of ETC inhibitors, complex V (i.e. F_1,F_0- ATPase or ATP synthetase), which normally uses the transmitochondrial [H^+] gradient to make ATP, can reverse direction and extrude H^+ by hydrolysing ATP imported from the cytosol via the adenine nucleotide translocase. To prevent this extra ATP hydrolysis and its effect on Ψ_m, complex V was sometimes inhibited by adding the phosphoryl transfer inhibitor oligomycin (10 μg ml^{-1}, Lardy *et al.* 1958) to the amytal-containing solution.

Action potentials were evoked in the motor nerve by applying brief (0.3 ms) suprathreshold depolarizing pulses via a suction electrode. Stimulation consisted of trains of 1000–2500 stimuli at 50 Hz, unless otherwise noted. Intertrain intervals were at least 10 min, to ensure return of mitochondrial [Ca^{2+}] to baseline levels (David, 1999). Before each experiment, the viability of the preparation was confirmed by observing muscle contractions during 1 Hz stimulation. Muscle contractions were then blocked using 15 μM tubocurarine, which blocks cation flux across postsynaptic nicotinic acetylcholine receptors. Thus the stimulation-induced fluorescence changes measured here did not originate from the muscle endplate.

Measurement of stimulation-induced changes in NADH and FAD^+ autofluorescence

NADH (excitation, 360 nm; emission, 460 nm) is much more fluorescent than its oxidized form (NAD^+, see spectra in Fig. 1 of Mayevsky & Rogatsky, 2007). The emission spectra of NADH (mainly mitochondrial) and NADPH (mainly cytosolic) are similar; the stimulation-induced changes recorded here probably arose mainly from NADH. $FADH_2$, which carries reducing equivalents from the TCA cycle to complex II of the ETC, is much *less* fluorescent than its oxidized form FAD^+ (excitation, 450 nm; emission, > 500 nm).

To reduce background fluorescence we selected neuromuscular junctions situated on the edge of the muscle fibre. In most cases muscle cytosol was cleared from the endplate region, as described by David (1999). Briefly, the preparation was incubated in 0.25 mg trypsin (ml NLS)$^{-1}$ for 3 min. After 30 s of trypsin exposure, muscle fibres were cut at a region remote from end plates using a glass pipette, and then the trypsin was washed out. This procedure caused muscle proteins to contract and clump within the muscle membrane sheath. We selected terminals in which this procedure had cleared most cytosolic proteins from the endplate region. These terminals continued to release transmitter [as assayed by destaining of preloaded FM1-43 (Cochilla *et al*. 1999); data not shown], and their changes in matrix and cytosolic [Ca^{2+}] during stimulation were similar to those recorded in terminals innervating intact muscle (David, 1999).

Stimulation-induced changes in NADH fluorescence were usually small. The magnitude of the recorded change probably depended in part on the amount of non-terminal, non-responding tissue (e.g. muscle remnants) included within the analysed regions of interest. We selected terminals that yielded detectable (> 5%), reversible, stimulation-induced changes in NADH fluorescence that were stable under control conditions. In such terminals, responses to multiple stimulus trains could often be recorded stably for several hours (average 3.3 h for 21 terminals).

Measurement of stimulation-induced changes in Ψ_m

Changes in Ψ_m were measured using rhodamine 123 (Rh123), a cell-permeant, cationic, fluorescent dye that

is readily sequestered by viable mitochondria. A 30 min incubation in 3 μg ml^{-1} Rh123 allowed sufficient uptake of Rh123 into the matrix to self-quench. Rh123 was then removed from the bath by repeated rinsing in NLS for 30 min. Excitation was at 488 nm; emission was detected using a 40 nm bandpass filter centred at 535 nm (Chroma, Rockingham, VT, USA). Depolarization of Ψ_m caused Rh123 to leak out of mitochondria into the cytosol where Rh123 became unquenched, producing an increase in fluorescence (reviewed by Nicholls & Ward, 2000). This interpretation is supported by the data of Fig. 3*A*, which show an increase in Rh123 fluorescence following application of cyanide, which depolarizes mitochondria by blocking complex IV of the ETC (Van Buuren *et al.* 1972).

The overlap between excitation and emission wavelengths used for FAD^+ autofluorescence and Rh123 fluorescence did not significantly affect measurements of Ψ_m depolarization, because emissions from FAD^+ were much less intense than those from Rh123. This was demonstrated in an experiment in which stimulation-induced changes in NADH and FAD^+ fluorescence were monitored in a terminal during successive stimulus trains. The terminal was then loaded with Rh123 for 10 min (shorter than the standard 30 min exposure to Rh123), after which Rh123 was washed out. Calculations of FAD^+ fluorescence during stimulation and of *resting* Rh123 fluorescence for the same light exposure times and terminal regions (i.e. those regions in which NADH fluorescence decreased during stimulation) indicated that the FAD^+ signal was less than 0.1% of the Rh123 signal.

Measurement of stimulation-induced increases in mitochondrial and cytosolic [Ca^{2+}]

Changes in mitochondrial [Ca^{2+}] in motor terminals were measured as described by David *et al.* (2003) using Xrhod-5F (K_d, ~1.6 μM; excitation, 568 nm; emission, > 590 nm, long-pass filter, Chroma). Preparations were incubated with the acetoxymethyl ester (AM) derivative of Xrhod-5F dissolved in NLS (final concentration, 25 μg ml^{-1}) for 15–20 min, followed by rinsing in indicator-free NLS for 30 min. Esterases in the cytosol and organelles (e.g. mitochondria) cleave off the AM moiety, trapping the indicator within the cell. With this loading protocol the concentration of indicator in motor terminal cytosol is low, probably because as the AM derivative is washed out of the bath, most of the indicator in the cytosol diffuses out of the terminal into the large volume of the attached motor axon. (Perineurial and myelin sheaths prevent the axon from taking up the AM derivative from the bath.) Thus most of the indicator remaining in the terminal is contained within compartments such as mitochondria. The mitochondrial origin of most of the stimulation-evoked fluorescence changes was confirmed by the following morphological, pharmacological and kinetic criteria. First, the fluorescence increase following trains of stimuli was punctate and localized within the nerve terminal, consistent with the known clustering of mitochondria within motor terminals. Second, the stimulation-induced increase in fluorescence was abolished by Ψ_m depolarizing agents. Third, mitochondrial [Ca^{2+}] decayed slowly when stimulation ceased (see Fig. 4), with little or none of the rapid initial decay characteristic of cytosolic [Ca^{2+}] (David *et al.* 1998; David, 1999; García-Chacón *et al.* 2006). Non-mitochondrial organelles within the terminal may also contain the indicator, but apparently do not undergo stimulation-induced [Ca^{2+}] changes over the concentration range detected by the indicator. For example, stimulation-induced fluorescence responses were not significantly altered by drugs that block endoplasmic reticular Ca^{2+} pumps or Ca^{2+} release channels (David, 1999).

Cytosolic [Ca^{2+}] was measured using fluo-4 dextran (molecular weight, 10 000; K_d, ~4 μM; excitation, 488 nm, emission detected using a 40 nm bandpass filter centred at 535 nm, Chroma). This indicator was loaded into the terminal by incubating the cut end of a 2–3 mm length of nerve trunk for 24 h in a small well (1 ml) containing a saturated solution of the dye (see Narita *et al.* 1998).

Image collection and analysis

The fluorescence of the indicators for Ψ_m and cytosolic and mitochondrial [Ca^{2+}] was measured using a sensitive confocal microscope system that included a Yokogawa spinning disc (Solamere, Salt Lake City, UT, USA), a Photometrics Cascade 512B CCD camera (Roper Scientific, Trenton, NJ, USA) and an argon-krypton laser (Laser Physics, Salt Lake City, UT, USA). To reduce photodamage, laser excitation light was reduced to < 0.05 mW using a 1% transmission neutral density filter. The ultraviolet and blue wavelengths used to excite NADH and FAD^+ came from a monochromator (Delta Ram V, Photon Technology International, Birmingham, NJ, USA) rather than a laser, so these measurements were not confocal.

Data were recorded using IP Lab v3.61 software (Scanalytics, Inc., Fairfax, VA, USA). Software macros allowed alternating collection of images at multiple wavelengths (as in Fig. 4*A*). Data were analysed on a Pentium computer using V^{++} software (Digital Micro Optics, Auckland, New Zealand). Regions of interest were outlined to include terminal regions whose fluorescence changed during stimulation. After subtracting background fluorescence, normalized fluorescence was plotted as F/F_0, where F is fluorescence and F_0 is the averaged resting

fluorescence prior to stimulation (except in Fig. 1*A*, where data were plotted as the change in fluorescence (ΔF) divided by F_0). Images were collected with exposures of 0.8–1.5 s at intervals of 3 s (single wavelength) or 5 s (dual wavelength), unless otherwise noted.

Average values are reported as means ± S.E.M. Data were plotted using Prism (version 3, Graph Pad Software, San Diego, CA, USA). In some cases (e.g. Figs 1*D* and *E* and 2) curves were fitted to data points using a weighted average of the 13 nearest neighbours.

Reagents

Fluorescent indicators were purchased from Molecular Probes (now Invitrogen, Carlsbad, CA, USA; excitation and emission spectra can be found on their website). ω-conotoxin GVIA (ω-CTX) was from Alomone Laboratories (Jerusalem, Israel) and botulinum toxin A from Wako Chemicals USA (Richmond, VA, USA). Other reagents were from Sigma (St Louis, MO, USA).

Results

The stimulation-induced decrease in NADH fluorescence requires Ca^{2+} influx into motor terminals

Figure 1*A–C* presents evidence that the NADH and FAD^+ fluorescence signals recorded from motor terminals originated from mitochondria. Stimulation at 50 Hz

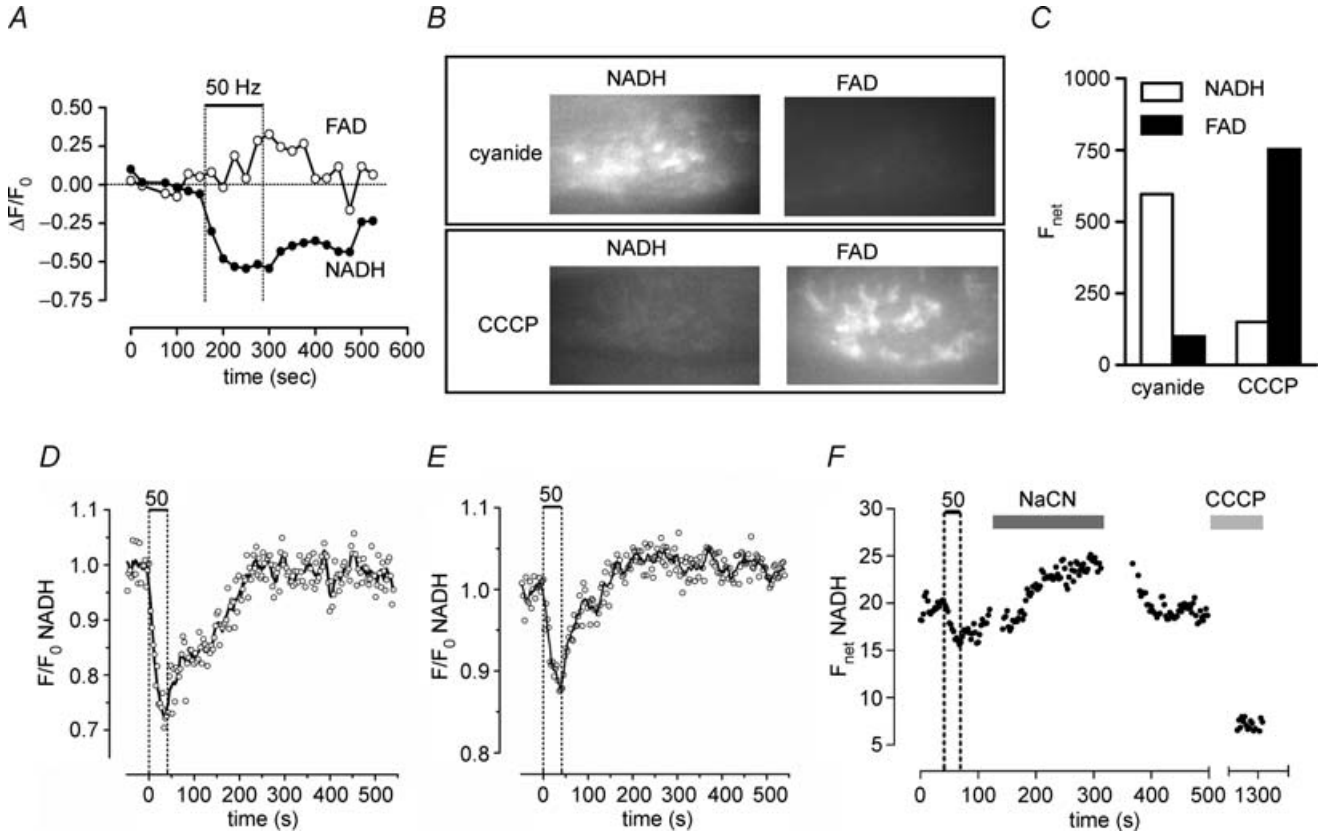

Figure 1. Stimulation of lizard motor terminals evokes a reversible decrease in NADH autofluorescence
A, decrease in NADH fluorescence and increase in FAD^+ fluorescence (change in ratio of fluorescence to the averaged resting fluorescence prior to stimulation; $\Delta F/F_0$) induced by 100 s of 50 Hz stimulation in a terminal. Vertical dashed lines mark the beginning and end of the stimulus train, which was longer than the trains used in subsequent figures. The sampling rate was 2.3 min^{-1}. *B* and *C*, reciprocal changes in net fluorescence (arbitrary units) of NADH and FAD^+ in a terminal exposed first to 2 μM CCCP to induce maximal oxidation and then to 10 mM cyanide to induce maximal reduction of mitochondrial pyridine nucleotides. *D* and *E*, two patterns of NADH fluorescence (F/F_0) change evoked by 50 s of 50 Hz stimulation. In the terminal in *D*, NADH fluorescence simply returned to baseline following stimulation, whereas in the terminal in *E* there was a small, prolonged poststimulation increase in NADH fluorescence. *F*, changes in net NADH fluorescence in a terminal that was (in succession) stimulated at 50 Hz, exposed to Na cyanide to maximize NADH, returned to normal medium, and exposed to CCCP to minimize NADH fluorescence ($n = 3$ experiments). Image collection was discontinued during solution changes; points between 500 and 1250 s are not shown. Data in *A–C* were collected with an imaging system that included a Leica DM IRBE fluorescence microscope, a TILL Photonics monochromator, and a Hamamatsu ER CCD camera. Data in *D–F* and all subsequent figures were obtained using the imaging system described in the Methods.

reversibly decreased NADH fluorescence and increased FAD^+ fluorescence (Fig. 1*A*). In unstimulated terminals, net NADH flourescence was much greater in the presence of 10 mM cyanide (a complex IV inhibitor that induces maximal reduction of mitochondrial pyridine nucleotides) than in 2 μM carbonyl cyanide m-chlorophenylhydrazone (CCCP, a proton carrier that induces maximal oxidation; Cunarro & Weiner, 1975). The converse was true for FAD^+ fluorescence, which was greater in the presence of CCCP than cyanide (Fig. 1*B* and *C*). Thus stimulation induced a net oxidizing shift, decreasing NADH and increasing FAD^+ fluorescence. In subsequent experiments, only NADH fluorescence was used to assess oxidation–reduction status because with the imaging protocols and 20–40 s stimulus trains used in Figs 2–6, the relatively small stimulation-induced changes in FAD^+ fluorescence were hard to detect.

NADH fluorescence remained low during stimulation, and began to increase as soon as stimulation stopped. In most terminals (20 of 23 in NLS), NADH fluorescence returned monophasically to baseline levels, usually within 5 min after the end of stimulation (Fig. 1*D*). The remaining terminals showed a delayed poststimulation increase in NADH fluorescence (Fig. 1*E*). The magnitude of this increase was always smaller than that of the initial decrease during stimulation. This pattern of NADH changes is quite different from that measured following stimulation of most other tissues, where the dominant change is a slow, prolonged increase in NADH fluorescence (references in Introduction and Discussion).

One possible explanation for a small or absent poststimulation NADH overshoot is that NADH might already be almost maximally reduced in the resting terminal. The experiment illustrated in Fig. 1*F* tested this possibility. Here, a terminal was first stimulated in physiological saline to confirm viability. Subsequent application of cyanide produced a clear increase in net NADH fluorescence, the absolute magnitude of which was comparable to that of the stimulation-induced decrease in NADH fluorescence. Following washout of cyanide, application of CCCP reduced NADH fluorescence to basal levels. These results suggest that NADH is not maximally reduced in resting terminals.

Figure 2*A* shows that the stimulation-induced decrease in NADH fluorescence was Ca^{2+}-dependent, because it was abolished by the Ca^{2+} chelator BAPTA. As action potential propagation into motor terminals persists in the presence of a low bath [Ca^{2+}] (Angaut-Petit *et al.* 1989), this result indicates that Na^+ influx and/or the resulting Na^+–K^+-ATPase activity are not sufficient to produce the stimulation-induced changes in NADH fluorescence. Figure 2*B* shows that the stimulation-induced decrease in NADH fluorescence was inhibited by ω-CTX (3 μM). ω-CTX blocks the N-type Ca^{2+} channels ($Ca_v2.2\alpha1$ or $\alpha1$B) that mediate stimulation-evoked increases in cytosolic [Ca^{2+}] and transmitter release in lizard motor terminals (Morita & Barrett, 1989; David *et al.* 1997). This result links the stimulation-induced decrease in NADH fluorescence to motor terminals.

The partial depolarization of Ψ_m during repetitive stimulation is Ca^{2+}- (or Sr^{2+})-dependent

In other tissues, the initial decrease in NADH fluorescence during stimulation has been attributed to acceleration of ETC activity resulting from Ψ_m depolarization, which reduces the energy barrier that opposes ETC H^+ extrusion (e.g. Duchen, 1992). Consistent with this idea, Fig. 3*A*

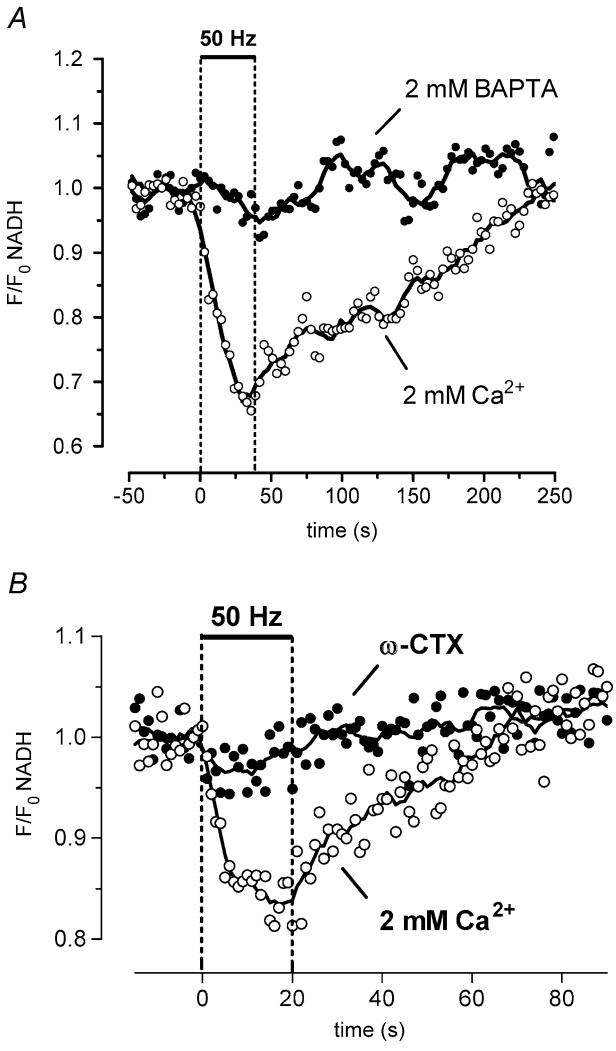

Figure 2. The stimulation-induced decrease in NADH autofluorescence depends on Ca^{2+} influx into motor terminals
The response to 50 Hz stimulation disappeared following addition of 2 mM BAPTA to reduce bath [Ca^{2+}] (*A*), or 3 μM ω-conotoxin GVIA (ω-CTX) to block N-type Ca^{2+} channels (*B*). Control and ω-CTX records in *B* are averages of four trials; ω-CTX records were obtained after 50–105 min of drug exposure. *A* and *B* were recorded from separate terminals; $n = 2$ experiments for both *A* and *B*.

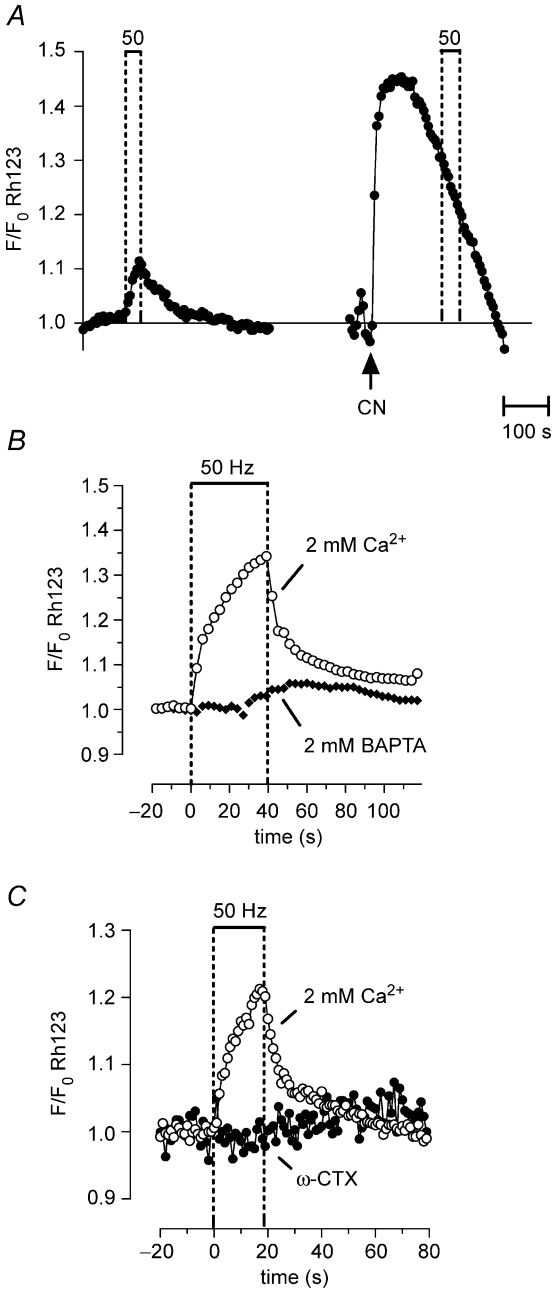

Figure 3. Repetitive stimulation produces a partial, reversible depolarization of Ψ_m that depends on Ca^{2+} influx into motor terminals

Ψ_m depolarization was indicated by an increase in Rh123 fluorescence (due to unquenching). *A*, Rh123 fluorescence changes in response to a 50 Hz, 40 s stimulus train (left), followed by addition of 1 mM cyanide (CN, right). A second 50 Hz stimulus train applied following CN exposure produced no further increase in fluorescence. The CN-induced fluorescence increase probably underestimated the CN-induced depolarization of Ψ_m, because of loss of Rh123 from the terminal via diffusion into the axon and bath (Nicholls & Ward, 2000). *B* and *C*, the stimulation-induced increase in Rh123 fluorescence was inhibited by adding 2 mM BAPTA (*B*) or 3 μM ω-conotoxin GVIA (ω-CTX) to the physiological saline (*C*). The illustrated stimulation-induced partial Ψ_m depolarization was not detected in a previous study (David, 1999) that used a less-sensitive imaging system. *A–C* were recorded from different terminals; $n = 1$ experiment for *A*; $n = 2$ experiments for *B* and *C*.

shows that in motor terminals repetitive stimulation transiently depolarized Ψ_m, as indicated by an increase in Rh123 fluorescence. This depolarization began to reverse as soon as stimulation ceased. Similar Rh123 fluorescence responses could be recorded repeatedly from the same terminal (see Figs 4*C* and 6*C*). The Ψ_m depolarization was only partial, because later application of cyanide to this terminal produced a much greater increase in Rh123 fluorescence (Fig. 3*A*). These data cannot be used to measure the magnitude of the stimulation-induced Ψ_m depolarization, because the relationship between Ψ_m and Rh123 fluorescence is not linear.

The stimulation-induced partial depolarization of Ψ_m was inhibited by addition of 2 mM BAPTA (Fig. 3*B*), and by addition of ω-CTX (Fig. 3*C*). This Ca^{2+} dependence is consistent with the hypothesis that the Ψ_m depolarization is produced by Ca^{2+} influx into mitochondria (as hypothesized for other cells; Lotscher *et al.* 1980; Duchen, 1992; Loew *et al.* 1994; Bindokas & Miller, 1995; Schuchmann *et al.* 2000).

Figure 4*A* and *B* shows dual-imaging experiments comparing the time courses of the stimulation-induced changes in Ψ_m and NADH with the time course of changes in matrix $[Ca^{2+}]$ measured using Xrhod-5F loaded into terminal mitochondria as described in the Methods. Figure 4*A* shows that Ψ_m depolarization decayed rapidly once stimulation ended, but mitochondrial $[Ca^{2+}]$ decayed much more slowly. The single-train records in Fig. 4*B* (open symbols) show that the decrease in NADH fluorescence also decayed more rapidly than mitochondrial $[Ca^{2+}]$. Thus the time courses of the changes in both Rh123 and NADH fluorescence were linked more closely to the time course of stimulation than to the time course of mitochondrial $[Ca^{2+}]$.

We could not directly measure Ca^{2+} influx into mitochondria, but this influx is expected to drop sharply when stimulation stops because both cytosolic $[Ca^{2+}]$ and transmitter release decrease rapidly following stimulation (Fig. 6*D* and David *et al.* 1997, 1998; Talbot *et al.* 2003), and Ca^{2+} influx through the mitochondrial uniporter/channel varies as the 3.5 power of cytosolic $[Ca^{2+}]$ (for review see Nicholls, 2005). Based on this argument and the Ca^{2+} dependence demonstrated above, we hypothesize that the stimulation-induced Ψ_m depolarization and decrease in NADH fluorescence are both linked to Ca^{2+} influx into mitochondria.

The prolonged poststimulation decay of mitochondrial $[Ca^{2+}]$ is probably *not* due to continued Ca^{2+} influx into mitochondria. Rather, this slow decay appears to reflect a balance between Ca^{2+} extrusion via the mitochondrial Na^+–Ca^{2+} exchanger and Ca^{2+} dissociation from an insoluble complex containing calcium and phosphate, which contributes to the powerful, non-linear Ca^{2+} buffering system in the mitochondrial matrix (David, 1999; García-Chacón *et al.* 2006; see also measurements in isolated neuronal mitochondria by Chalmers & Nicholls,

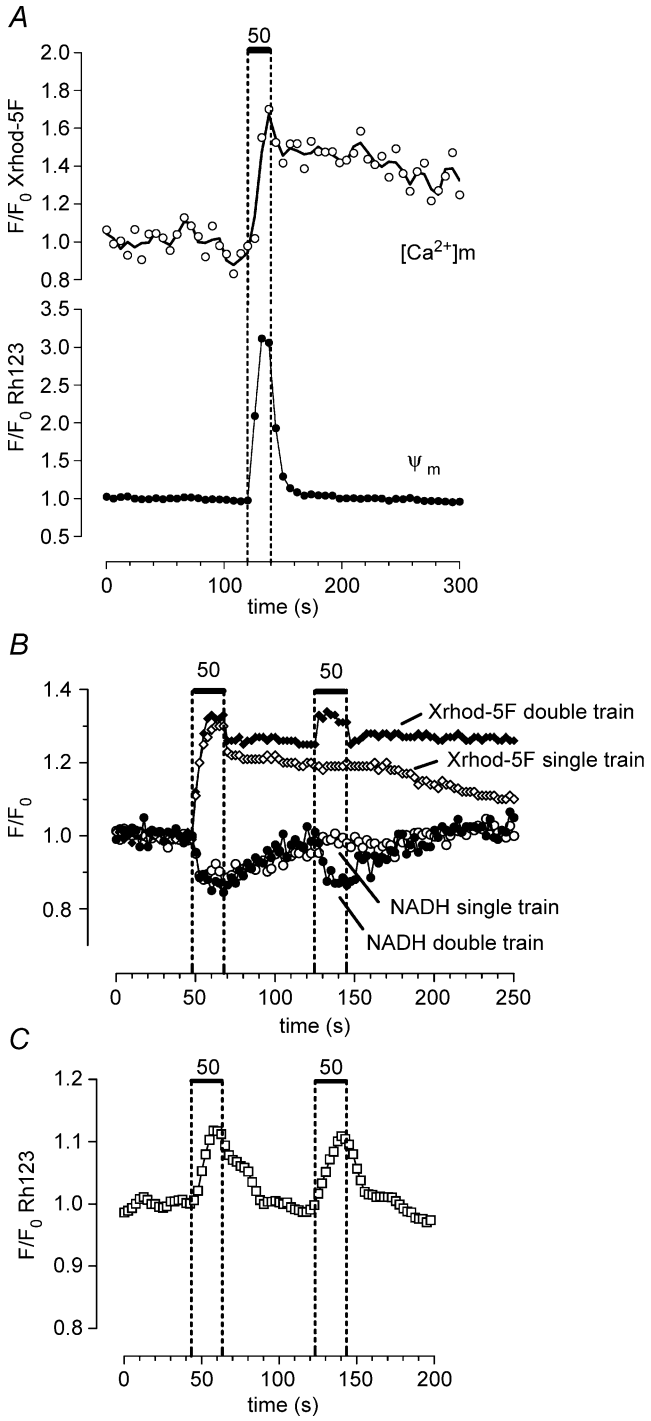

Figure 4. The stimulation-induced depolarization of Ψ_m and decrease in NADH fluorescence return to baseline faster than the increase in matrix [Ca^2]

Changes in matrix [Ca^{2+}] were measured using Xrhod-5F loaded into the mitochondrial matrix as described in the Methods. *A*, changes in mitochondrial [Ca^{2+}] (upper trace) and Ψ_m (lower trace) recorded simultaneously from the same motor terminal ($n = 2$ experiments). *B*, sequentially recorded changes in NADH fluorescence (circles, lower traces) and matrix [Ca^{2+}] (diamonds, upper traces) recorded from another terminal. Responses to a single 20 s train (open symbols) and two sequential 20 s trains (filled symbols) are superimposed. *C*, changes in Rh123 fluorescence recorded from a different terminal following a two-train stimulation pattern as in *B*. In *A* the stimulation-induced increase in Rh123 fluorescence was greater than that illustrated other figures. A likely explanation for this is that in this terminal the regions of interest in which Rh123 fluorescence was analysed were defined as those regions that showed a stimulation-induced increase in Xrhod-5F fluorescence. This procedure improved the spatial resolution and consequently the signal-to-noise ratio of the Rh123 signal by reducing the amount of Rh123 fluorescence recorded from non-responsive regions. In *B* the prolonged poststimulation plateau of Xrhod-5F fluorescence was not due to saturation of the indicator, but rather to the powerful matrix buffering system described in the text. In *B* the NADH records were collected first, then the mitochondrial matrix was loaded with Xrhod-5F; the small, rapid initial decay in Xrhod-5F fluorescence following each stimulus train may have arisen from a small amount of Xrhod-5F remaining in the cytosol.

2003; and see reviews by Carafoli, 2003; Nicholls, 2005). The rate of rise of the initial stimulation-induced elevation of matrix [Ca^{2+}] is likely to be determined mainly by conventional buffers, but the plateau during stimulation probably reflects the (reversible) formation of the abovementioned calcium–phospate complex. Formation of this complex during gradually administered Ca^{2+} loads such as those accompanying repetitive nerve stimulation, limits the elevation of mitochondrial [Ca^{2+}] to ~1–2 μM (David, 1999; David *et al.* 2003; Chalmers & Nicholls, 2003). Because resting matrix [Ca^{2+}] is estimated to be only ~0.1 μM, a 1–2 μM elevation of matrix [Ca^{2+}] following stimulation would not saturate Xrhod-5F (K_d, ~1.6 μM).

These considerations, combined with results described above in Figs 2, 3 and 4*A* and the single-train record of Fig. 4*B*, suggest that the stimulation-induced Ψ_m depolarization and decrease in NADH are more likely to be associated with influx of Ca^{2+} into the matrix during the stimulus train than with the presence of elevated matrix [Ca^{2+}]. This conclusion is supported by results of the double-train experiments in Fig. 4*B* and *C*. The second train, administered while matrix [Ca^{2+}] was still elevated following the first train, produced a decrease in NADH fluorescence (Fig. 4*B*) and a partial Ψ_m depolarization (Fig. 4*C*) similar to those recorded following the first train, even though the increase in matrix [Ca^{2+}] produced by the second train was smaller than that following the first train (Fig. 4*B*). Matrix [Ca^{2+}] decayed more slowly following the double train, consistent with findings by García-Chacón *et al.* (2006) that increasing the magnitude of the Ca^{2+} load delivered to mitochondria has little or no effect on maximal matrix [Ca^{2+}] (because of the non-linear buffering described above), but does prolong the decay of matrix [Ca^{2+}].

Figure 5*A* and *B* shows that the stimulation-induced decrease in NADH fluorescence and partial Ψ_m depolarization persisted when bath Ca^{2+} was replaced by

Sr^{2+}, which readily passes through plasmalemmal Ca^{2+} channels (Wakamori *et al.* 1998) and the mitochondrial uniporter/channel (Kirichok *et al.* 2004).

The hypothesis that Ψ_m depolarization is produced by Ca^{2+} entry into mitochondria could be tested more directly by selectively blocking the mitochondrial Ca^{2+} uniporter. However, ruthenium red and its active component Ru360, which block the mitochondrial uniporter (Matlib *et al.* 1998), were not suitable for this experiment, because in motor terminals and some other neuronal preparations these drugs have non-specific effects that include reducing influx through plasmalemmal Ca^{2+} channels and quenching of Rh123 fluorescence (Duchen, 1992; David, 1999). Thus instead we tested whether other known Ca^{2+}-dependent mechanisms might account for the Ψ_m depolarization.

Stimulation-induced NADH oxidation and Ψ_m depolarization do not require transmitter release

Another mechanism that might depolarize Ψ_m and thus reduce NADH fluorescence is a decrease in the cytosolic ATP/ADP ratio. Because a major result of elevating cytosolic $[Ca^{2+}]$ in motor terminals is to stimulate vesicular release (with subsequent energy-dependent vesicular recycling), we tested the effect of botulinum toxin A (BoTxA, 40 nM), which irreversibly blocks stimulation-induced quantal release by cleaving the 25 kDa synaptosomal-associated protein (Blasi *et al.* 1993). BoTxA does not block stimulation-induced Ca^{2+} influx into motor terminals (Gundersen *et al.* 1982), and stimulation-induced increases in mitochondrial $[Ca^{2+}]$ persisted in the presence of BoTxA (data not shown). Figure 5*C* and *D* shows that the stimulation-induced

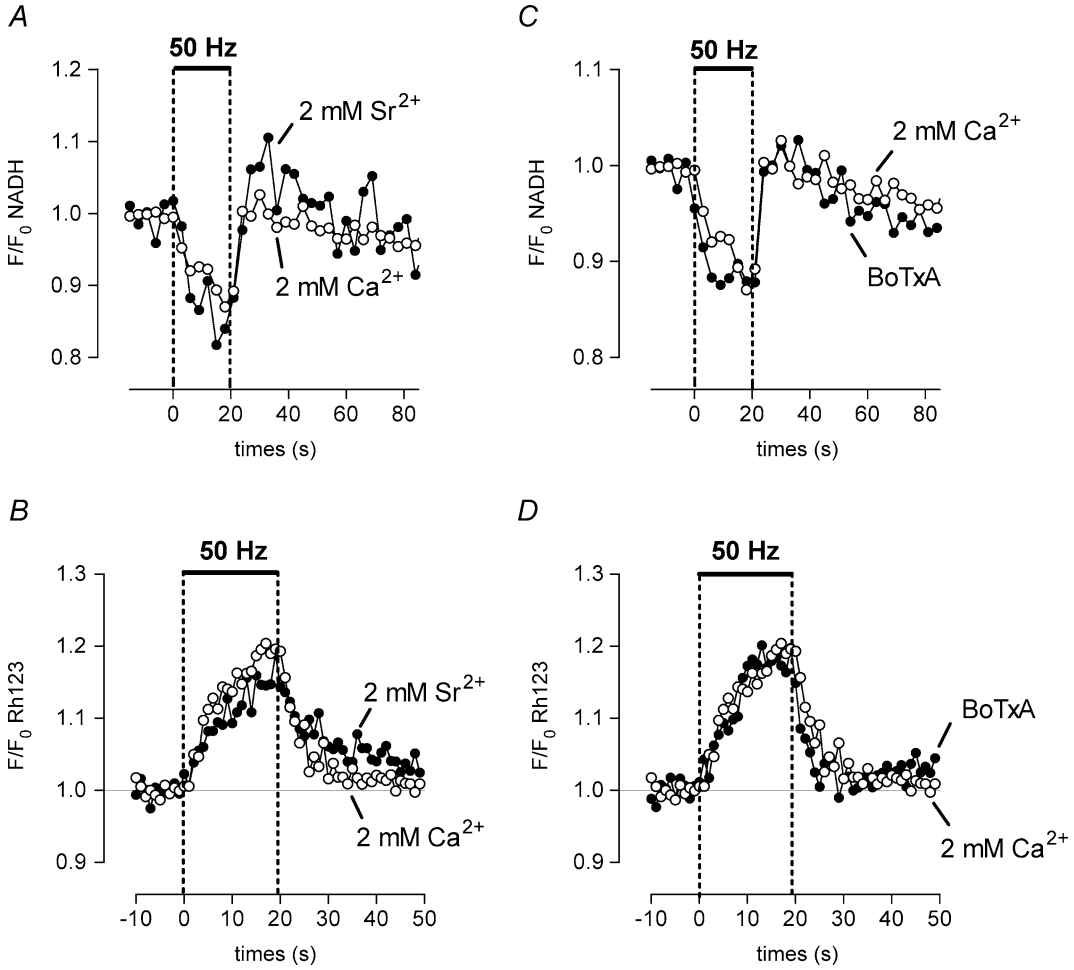

Figure 5. Effects of Sr^{2+} and botulinum toxin on stimulation-induced changes in NADH and Ψ_m
The stimulation-induced decrease in NADH autofluorescence and partial depolarization of Ψ_m persist when bath Ca^{2+} is replaced by 2 mM Sr^{2+} (*A* and *B*), and when transmitter release is blocked by 40 nM BoTxA (*C* and *D*). Records in *A* and *C* were recorded sequentially from the same terminal, and records in *B* and *D* from another terminal. $n = 3$ experiments for *A*–*C* $n = 1$ experiment for *D*.

oxidation of NADH and partial Ψ_m depolarization persisted after prolonged exposure to BoTxA. These results confirm that action potentials continued to be conducted into the motor terminal in the presence of BoTxA. To ensure that transmitter release was indeed inhibited by the toxin, tubocurarine was washed out of the bath to remove its blockade of postsynaptic acetylcholine receptors. Continued nerve stimulation did not produce muscle contraction, indicating that BoTxA had indeed blocked evoked transmitter release. Washout of tubocurarine from preparations not treated with BoTxA restored stimulation-evoked muscle contractions within 5–10 min (data not shown).

These experiments demonstrate that the rapid changes in NADH fluorescence and Ψ_m measured during stimulation do not require evoked quantal transmitter release. The persistence of these changes following equimolar replacement of Ca^{2+} by Sr^{2+} (Fig. 5*A* and *B*) is also consistent with this conclusion, as Sr^{2+} is less effective than Ca^{2+} at stimulating phasic transmitter release (Dodge *et al.* 1969; Meiri & Rahamimoff, 1971). Thus the acceleration of ETC activity suggested by the decrease in NADH fluorescence is not due to accelerated depletion of ATP as a consequence of vesicular release.

The results shown in Fig. 5*C* and *D* also confirm that the measured changes in NADH fluorescence and Ψ_m originated in motor terminals, because in the absence of quantal transmitter release, nerve stimulation is unlikely to have any rapid effects on either muscle fibres or perisynaptic Schwann cells.

The results shown in Figs 2 and 5 leave open the possibility that the stimulation-induced changes in NADH fluorescence might be influenced by changes in the ATP/ADP ratio produced by Ca^{2+}-dependent processes that are *not* linked to vesicular release and recycling. For any mechanism involving ATP depletion, one would expect the NADH response to be reduced by oligomycin, which inhibits ATP synthetase (complex V), and thus should block any stimulatory effect of a decreased ATP/ADP ratio on ETC activity. However, we found that instead of this predicted effect, oligomycin ($10\ \mu g\ ml^{-1}$) either did not change or actually increased the magnitude of the NADH response (compare filled and open circles in Fig. 6*A*). This result suggests that the stimulation-induced decrease in NADH fluorescence was *not* due to acceleration of ETC activity by a decreasing ATP/ADP ratio.

Compromised mitochondria exhibit greater stimulation-induced Ψ_m depolarization and reduced Ca^{2+} sequestration

Results thus far are consistent with the hypothesis that the reduction in NADH fluorescence measured during a stimulus train reflects an acceleration of ETC activity caused by the partial Ψ_m depolarization associated with Ca^{2+} influx into mitochondria. Because some neurological disorders are associated with impaired mitochondrial function (for review see DiMauro & Schon, 2003), we wondered how stimulation-induced changes in Ψ_m depolarization and mitochondrial Ca^{2+} sequestration would be altered in motor terminals in which the ability to accelerate ETC activity was pharmacologically impaired. In the experiments shown in Fig. 6, partial inhibition of complex I of the ETC was achieved using 5 mM amytal (see Methods). The inhibition was partial (rather than complete) because amytal produced little Ψ_m depolarization in resting terminals (data not shown), indicating that ETC activity remained sufficient to sustain Ψ_m at rest. Amytal reversibly abolished the stimulation-induced oxidation of NADH, both in the presence (Fig. 6*A*) and absence (Fig. 6*B*) of oligomycin. Oligomycin reduces the extra ATP depletion associated with F_1,F_0-ATPase activity during metabolic inhbition, as discussed in the Methods). Abolition of the NADH response in the presence of amytal suggests an inability to accelerate ETC activity in response to the Ca^{2+} influx-induced Ψ_m depolarization. This interpretation is supported by the data in Fig. 6*C*, which show that during stimulation in the presence of amytal and oligomycin, the depolarization of Ψ_m began earlier and reached a greater magnitude than in control solution.

Increased Ψ_m depolarization reduces the electrical gradient favouring Ca^{2+} influx into mitochondria, and thus would be expected to reduce mitochondrial Ca^{2+} sequestration. We cannot yet measure total Ca^{2+} uptake into motor terminal mitochondria, and measurements of matrix free $[Ca^{2+}]$ are unreliable indicators of partial inhibition of mitochondrial Ca^{2+} uptake during metabolic inhibition, due to the pH dependence (Chalmers & Nicholls, 2003) and highly non-linear nature of the matrix Ca^{2+} buffering mechanisms described above. Thus we tested the above prediction indirectly, by measuring changes in cytosolic $[Ca^{2+}]$, because mitochondrial Ca^{2+} uptake is the major mechanism that limits stimulation-induced elevations of cytosolic $[Ca^{2+}]$ in these terminals (David, 1999). Figure 6*D* shows that the stimulation-induced elevation of cytosolic $[Ca^{2+}]$ was markedly increased in the presence of amytal and oligomycin. This effect was not due to oligomycin, because short-term (30 min) exposure to oligomycin has little or no effect on stimulation-induced elevations of cytosolic $[Ca^{2+}]$ (David, 1999).

Thus these results support the hypothesis that terminals in which mitochondria have only a limited ability to accelerate ETC activity (at least via complex I) exhibit greater Ψ_m depolarization and reduced total mitochondrial Ca^{2+} sequestration during stimulation.

Discussion

Recordings presented here demonstrate that in motor nerve terminals repetitive nerve stimulation produces a Ca^{2+}-dependent partial depolarization of Ψ_m accompanied by oxidation of NADH. Following stimulation, NADH recovers to resting levels with no or minimal overshoot. Because these responses persisted when muscle acetylcholine receptors were blocked by tubocurarine and when transmitter release was blocked by BoTxA, the recorded Ψ_m and NADH changes must have arisen from motor terminals rather than from other cells influenced by released acetylcholine or ATP (e.g. muscle remnants or perisynaptic Schwann cells). To our knowledge, these are the first such measurements made on a single presynaptic terminal during application of physiological stimuli.

The stimulation-induced depolarization of Ψ_m is caused by Ca^{2+} influx across mitochondrial membranes, rather than a decrease in the ATP/ADP ratio

The partial depolarization of Ψ_m evoked by nerve stimulation could be caused by a decreased rate of H^+ extrusion via the ETC. For example, Sadek *et al.* (2004) suggested Ca^{2+}-dependent inhibition of complex I activity in isolated cardiac mitochondria. However, this mechanism is unlikely to mediate the Ψ_m depolarization

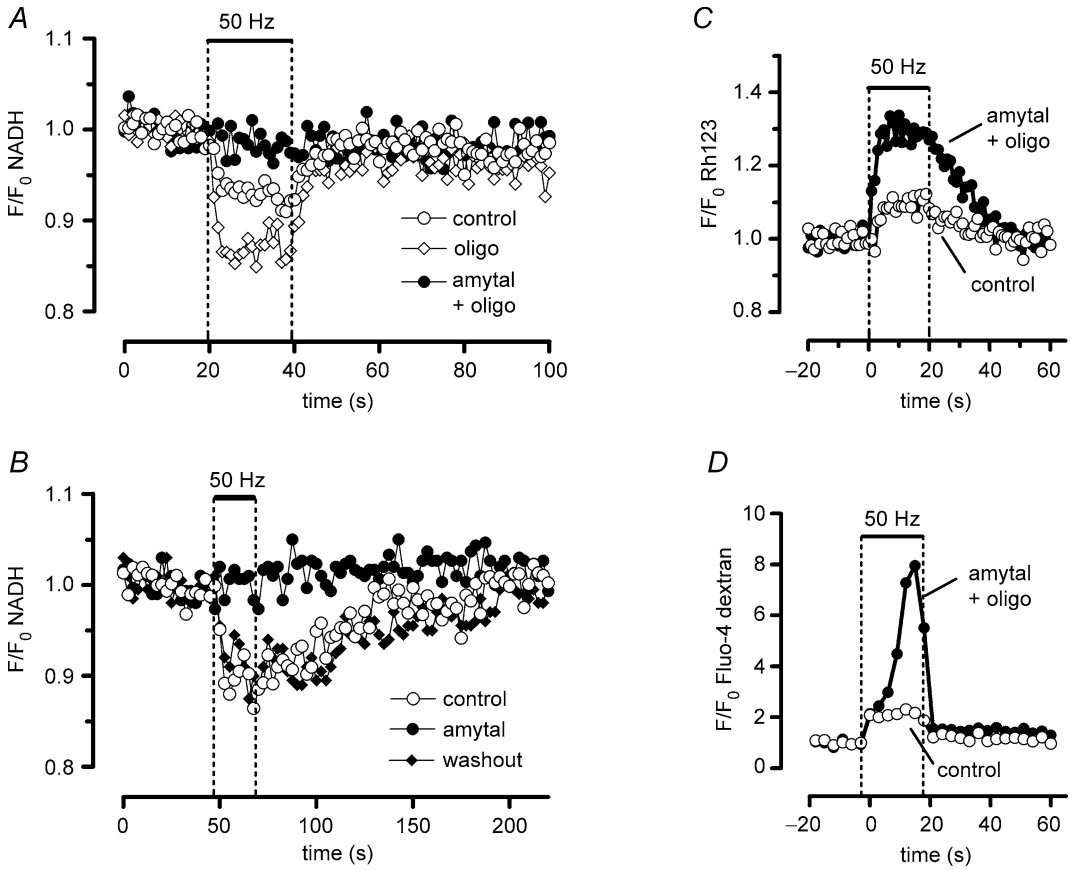

Figure 6. Effects of oligomycin and amytal on stimulation-induced changes in NADH, Ψ_m and cytosolic (Ca^{2+})

Partial inhibition of complex I activity with 5 mM amytal (●) changes motor terminal responses to stimulation by inhibiting the decrease in NADH fluorescence (A and B), increasing Ψ_m depolarization (*C*) and increasing the elevation of cytosolic [Ca^{2+}] (*D*). Amytal solutions also contained 10 μg ml^{-1} oligomycin in *A*, *C* and *D*. *A*, brief exposure to oligomycin alone (◇) increased the stimulation-induced decrease in NADH fluorescence; this effect was observed in 2 out of 3 experiments. The NADH response to stimulation gradually disappeared during the second hour of oligomycin exposure (not shown). *B*, the amytal-induced inhibition of the NADH response to stimulation is reversible. *C*, amytal increases Ψ_m depolarization during stimulation (averages from four to five trains recorded in two terminals in the same preparation). *D*, amytal increases the stimulation-induced elevation of cytosolic [Ca^{2+}] in a terminal in which the cytosol was filled with fluo-4 dextran. Amytal produced a slight increase in prestimulation net fluorescence in this terminal (data not shown). In *A*–*D* drugs were present for ≥ 20 min before the illustrated records were taken.

observed in motor terminals, because NADH fluorescence decreased (rather than increased) during stimulation. Also, the matrix [Ca^{2+}] required for complex I inhibition ((IC_{50}, ~10 μM) exceeds that measured in stimulated motor nerve terminals (1–2 μM, David *et al.* 2003).

Vergun & Reynolds (2005) described Ca^{2+}-dependent Ψ_m depolarizations in isolated brain mitochondria, which they attributed to transient transformation of the adenine nucleotide translocator into a non-specific pore. However their depolarization had a time course much slower than that of the rapidly developing, rapidly decaying Ψ_m depolarization studied here. Also the time course of the Ψ_m depolarization studied by Vergun & Reynolds (2005) was different in the presence of Sr^{2+} than in Ca^{2+}, whereas the time course of the stimulation-induced Ψ_m depolarization studied here was similar in the presence of either of these two divalent cations.

Mitochondrial export of ATP in exchange for ADP via the adenine nucleotide transporter is also electrogenic, and thus might contribute to stimulation-induced Ψ_m depolarization. However, any such contribution was probably minor, because Ψ_m repolarized rapidly following the stimulus train, even though the ATP-requiring restorative processes as a consequence of repetitive stimulation (e.g. Na^+ extrusion or endocytosis of vesicular membranes) occur over a longer time course. Also, the stimulation-induced Ψ_m depolarization persisted in the presence of oligomycin (Fig. 6*C*), which would reduce the amount of matrix ATP available for export.

The observed Ca^{2+}- (or Sr^{2+}-)dependent depolarization of Ψ_m combined with a decrease in NADH fluorescence could be caused by increased H^+ influx via complex V (ATP synthetase) due to a decreased cytosolic ATP/ADP ratio (respiratory control), and/or to increased Ca^{2+} influx into mitochondria. Evidence for accelerated ETC activity as a result of accelerated cytosolic ATP hydrolysis has been obtained (e.g. in heart muscle, where contractions consume ATP, Brandes & Bers, 2002; Jo *et al.* 2006). However, our data suggest that changes in the ATP/ADP ratio did not contribute strongly to acceleration of ETC activity during the stimulus trains employed here, because the NADH response was not reduced by the ATP synthetase blocker oligomycin, which should eliminate any effect of a changing ATP/ADP ratio on ETC activity. Instead, oligomycin sometimes *increased* the amplitude of the NADH response. Because oligomycin inhibits H^+ influx via ATP synthetase, it tends to hyperpolarize Ψ_m, which would reduce baseline (prestimulation) ETC activity. The resulting increase in baseline NADH might account for the observed greater magnitude of the recorded stimulation-induced decrease in NADH fluorescence.

The most likely explanation for stimulation-induced Ψ_m depolarization accompanied by decreased NADH fluorescence is Ca^{2+} influx into mitochondria (see 'Normal' side of diagram in Fig. 7). Supporting this hypothesis, the stimulation-induced changes in both NADH fluorescence and Ψ_m: (1) were inhibited by blocking the major voltage-dependent Ca^{2+} channel expressed in these terminals; (2) could be recorded in the presence of either Ca^{2+} or Sr^{2+}, which enter motor terminals and mitochondria via similar routes; and (3) began decaying as soon as stimulation (and thus Ca^{2+} influx) ended. This mechanism is similar to that proposed by others to explain high [K^+]-induced decreases in NADH fluorescence in neuronal somata (Duchen, 1992; Hayakawa *et al.* 2005) and neuroblastoma cells (Loew *et al.* 1994).

The decrease in NADH fluorescence in stimulated motor terminals may be especially large and sustained because the mitochondrial Ca^{2+} influx in these terminals exceeds that in other presynaptic terminals. In motor terminals, mitochondrial uptake becomes evident when average cytosolic [Ca^{2+}] has increased by only ~200 nM (David *et al.* 1998). By contrast, mitochondrial Ca^{2+} uptake is quantitatively less important at the calyx of Held (see Fig. 3 in Billups & Forsythe, 2002). In the calyx of Held, elevations in cytosolic [Ca^{2+}] of up to 2.5 μM are cleared mainly (91%) by plasma membrane mechanisms (Na^+–Ca^{2+} exchanger and Ca^{2+}-ATPase); mitochondrial contributions become significant (~25%) only with cytosolic [Ca^{2+}] elevations of 3–5 μM (Kim *et al.* 2005).

Stimulation-induced changes in NADH fluorescence and Ψ_m persisted in the presence of BoTxA, indicating that the Ca^{2+}-dependent mechanism(s) underlying the NADH and Ψ_m responses do not require transmitter release. This result is somewhat perplexing, because vesicular recycling would be expected to reduce the ATP/ADP ratio and thus alter mitochondrial function. One possible explanation is that over the brief intervals studied here, vesicular recycling consumes relatively little ATP. Current hypotheses suggest that hydrolysis of ATP (and/or GTP) is involved more in the slower events preceding and following release (e.g. vesicular filling, priming, docking, mobilization, endocytosis of vesicular membrane and restoration of transmembrane ion gradients) than in Ca^{2+}-triggered release of docked, primed vesicles (e.g. Sørensen, 2004; Mozhayeva *et al.* 2004). This idea is consistent with previous findings that short-term blockade of mitochondrial ATP synthesis with oligomycin has little or no effect on elevations of cytosolic or mitochondrial [Ca^{2+}] or on phasic or asynchronous quantal transmitter release evoked by 50 Hz stimulation (David, 1999; Talbot *et al.* 2003). Another possible explanation is that ATP hydrolysis is indeed increased by tetanic stimulation over the intervals studied here, but that ATP is rapidly replenished by glycolysis and/or by diffusion from the motor axon.

Why is the stimulation-induced increase in NADH fluorescence so small in motor terminals?

In most other tissues, including neuronal somata, chromaffin cells and neurohypophysial terminals (Duchen, 1992; Kann *et al.* 2003; Kosterin *et al.* 2005; Warashina, 2006), the most dramatic stimulation-induced change in NADH fluorescence is a prolonged increase (see additional references in the Introduction). This increase in NADH fluorescence is usually attributed to stimulation of the TCA cycle via Ca^{2+}-mediated stimulation of matrix dehydrogenases (see Introduction). However, in most motor terminals NADH simply recovered to prestimulation levels following stimulation, with little or no net increase, even though matrix $[Ca^{2+}]$ was clearly increased. The Ca^{2+}-dependent matrix dehydrogenases are maximally stimulated by only modest elevations of matrix $[Ca^{2+}]$ (in the nanomolar to low micromolar range, McCormack *et al.* 1990; Hansford, 1994). Perhaps resting matrix $[Ca^{2+}]$ in motor terminal mitochondria is sufficient for near maximal stimulation of these dehydrogenases. Regulation of matrix dehydrogenases may be more dependent on stimulation in cells where elevations of mitochondrial $[Ca^{2+}]$ are brief and modest (e.g. 700 nM in heart, Brandes & Bers, 1997, 2002; Jo *et al.* 2006) than in motor terminals, where stimulation-induced elevations of mitochondrial $[Ca^{2+}]$ can be greater and more sustained (e.g. see review by Nicholls, 2005).

Another possible explanation for the absence of a large stimulation-induced increase in NADH fluorescence is that NADH is the dominant form of NAD^+/NADH in resting motor terminals. Our finding that application of cyanide to a resting terminal produced a sizeable increase in the NADH signal would seem to argue against this explanation. However, this finding carries an important caveat: changes in NADH fluorescence produced by nerve stimulation originated mainly from motor terminals, but cyanide-induced changes originated from all cells in the region, including perisynaptic Schwann cells and any remaining muscle. Thus it remains possible that most of the cyanide-induced increase in NADH fluorescence originated from mitochondria in these other cell types.

The poststimulation increase in NADH fluorescence might also be minimal if NADH-producing and NADH-consuming reactions are evenly balanced. For example, the increased production of NADH predicted by elevated matrix $[Ca^{2+}]$ may help to restore NADH to its

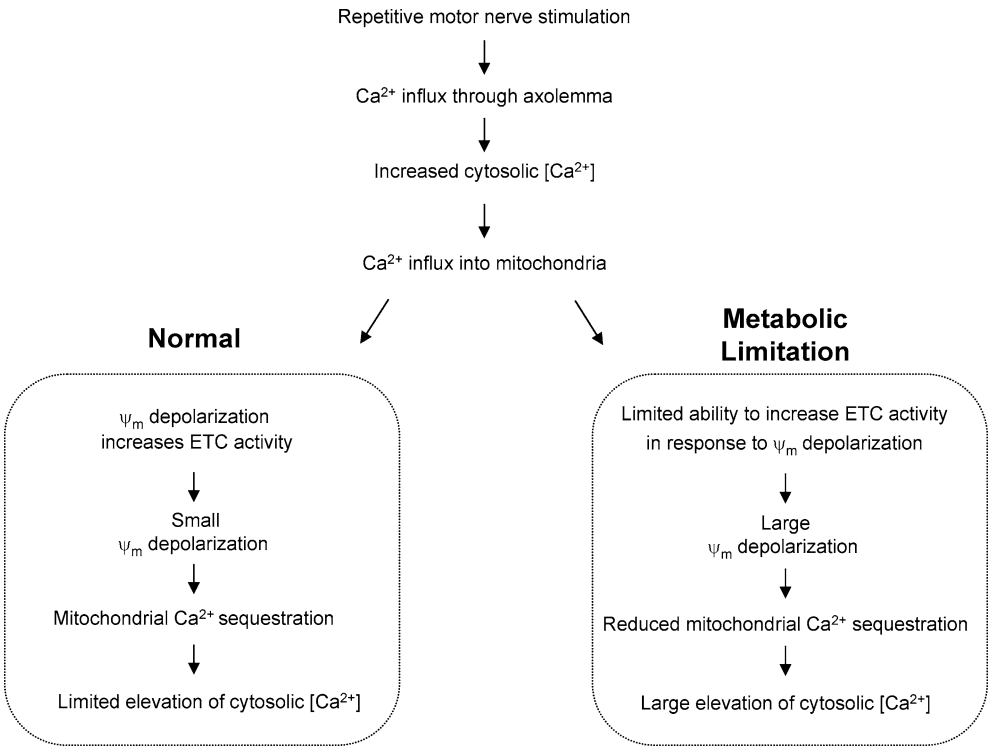

Figure 7. Hypothesized mechanism to explain experimental observations during repetitive stimulation under normal conditions (left box) and following amytal-induced partial inhibition of electron transport chain (ETC) activity (right box)
Sequential processes above the boxes are common to both conditions; divergence occurs as a result of differing extents of acceleration of ETC activity in normal and inhibited mitochondria in response to the Ψ_m depolarization produced by Ca^{2+} influx. This proposed mechanism helps to explain why repetitive nerve stimulation produced greater Ψ_m depolarization and greater elevation of cytosolic $[Ca^{2+}]$ in the presence of amytal.

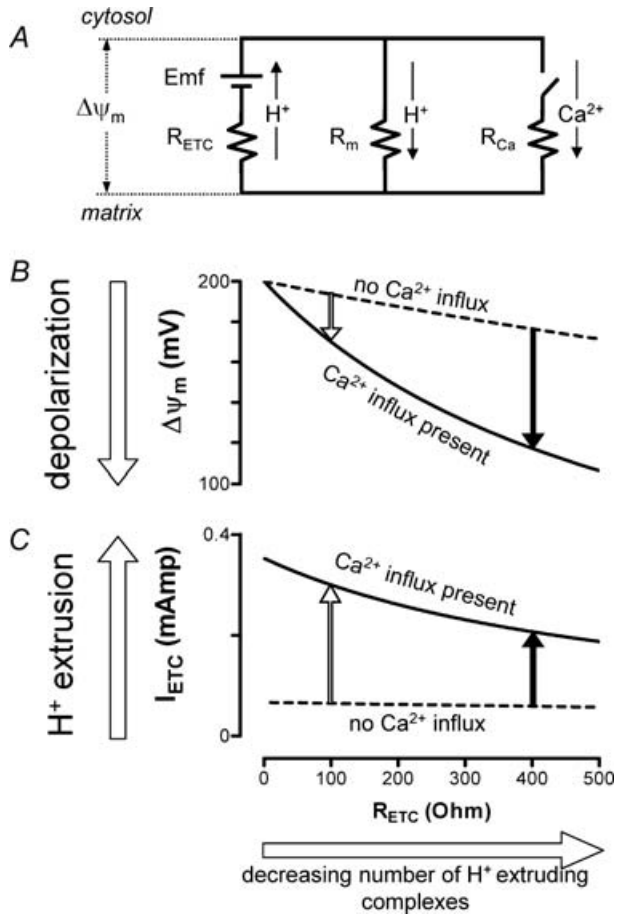

Figure 8. Partial inhibition of ETC activity has a greater effect on mitochondrial function in stimulated than in resting terminals
Simplified equivalent circuit of the mitochondrial inner membrane (*A*) allows prediction of how the number of H^+-extruding complexes affects Ψ_m depolarization (*B*) and ETC H^+ extrusion (*C*) in the absence (rest) or presence (stimulated) of Ca^{2+} influx into motor terminal mitochondria. Partial inhibition of ETC activity (e.g. due to inhibiting complex I) reduces the stimulation-induced increase in H^+ extrusion and increases the stimulation-induced depolarization of Ψ_m. In *A*, H^+ extrusion by respiratory complexes I, III and IV is modelled as current through R_{ETC} driven by the battery electromotive force (Emf), where R_{ETC} is the resistance of all proton-extruding complexes arranged in parallel. H^+ current into the matrix via H^+ leak and the F_1,F_0-ATPase (complex V) occurs via membrane resistance (R_m). Nerve stimulation is simulated by closing the switch in the Ca^{2+} branch of *A*, allowing Ca^{2+} to flow into the mitochondrial matrix via the uniporter (R_{Ca}). In *B* and *C*, a reduction in the number of active complexes is simulated by increasing R_{ETC}. The length of the vertical arrows in *B* and *C* indicates the magnitude of the changes in Ψ_m and I_{ETC} (respectively; I_{ETC} is current through ETC complexes) associated with Ca^{2+} influx into inhibited (filled arrows) and non-inhibited (open arrows) mitochondria. *B* and *C* were calculated by applying Kirchoff's and Ohm's laws to this circuit [for *B*, $\Delta\Psi_m = Emf/(1 + R_{ETC}(R_m^{-1} + R_{Ca}^{-1})$; for *C*, $I_{ETC} = (Emf - \Delta\Psi_m)/(R_{ETC})$]. Parameters used in the simulations of *B* and *C* (adjusted for 1 mg protein) were Emf = 200 mV, $R_m = 3 \times 10^3\ \Omega$, $R_{Ca} = 7 \times 10^2\ \Omega$ (value at half-maximal conductance of the uniporter, Magnus & Keizer, 1997). R_{ETC} in normally respiring mitochondria is ~10 Ω (Nicholls, 1974). Capacitance (0.14 MF) was omitted because the time constant of this circuit is very short compared to the duration of Ca^{2+} influx. This simplified model ignores the chemical components of the driving forces for Ca^{2+} and H^+ fluxes, assumes no changes in the concentrations of substrate or these ions, and ignores possible changes in Emf (e.g. due to depletion of NADH) and possible saturation of respiratory chain complexes. A similar, albeit more complex, equivalent circuit has been presented by Lemeshko (2002).

resting level following stimulation, but any further increase may be offset by increased NADH consumption driven by an increased ATP/ADP ratio, as ATP (or GTP) is expended to recycle vesicles and restore plasma membrane ion balances. However, the absence of any detectable persisting Ψ_m depolarization following stimulation and the failure of oligomycin and BoTxA to produce a persisting net increase in NADH fluorescence, argue against major regulation driven by a change in the ATP/ADP ratio during or shortly after stimulation.

Thus at present we have no compelling explanation for the minimal poststimulation elevation of NADH in motor terminals.

The ability to accelerate ETC activity is necessary for sustained mitochondrial Ca^{2+} uptake during repetitive stimulation

The sustained mitochondrial Ca^{2+} influx that occurs in motor terminals during repetitive stimulation requires maintenance of a cytosol-to-matrix electrochemical gradient favouring Ca^{2+} influx. Accelerated H^+ extrusion by the ETC driven by Ψ_m depolarization should help sustain an electrical gradient. Consistent with this idea, we found that partial inhibition of complex I to limit the ability of the terminal to accelerate ETC activity resulted in increased Ψ_m depolarization, abolition of the decrease in NADH fluorescence, and greater elevation of cytosolic $[Ca^{2+}]$ during repetitive stimulation. A scenario linking these effects is shown in the 'Metabolic Limitation' box in Fig. 7.

These findings in motor terminals are reminiscent of those reported in central neurons, synaptosomes and isolated brain and synaptosomal mitochondria (Chinopoulos *et al.* 1999; Ward *et al.* 2000; Kanki *et al.* 2004; Votyakova & Reynolds, 2005). In all these studies, inhibitors of complex I had a much greater effect on Ψ_m and/or Ca^{2+} handling in stimulated than in resting preparations. Flux control coefficients measured by Davey *et al.* (1997) suggest that complex I has a greater impact on overall respiratory flux in synaptosomal than in non-synaptosomal mitochondria.

Figure 8 shows calculations based on a simplified electrical model of the inner mitochondrial membrane to explain why partial inhibition of ETC activity has a greater effect on Ψ_m and Ca^{2+} handling in stimulated than in resting cells. Fig. 8*A* includes a proton motive battery in which the electromotive force (Emf) is generated by the ETC using the redox potential difference between NAD^+/NADH and O_2/H_2O. This Emf drives H^+ current

(I_{ETC}) across the resistance of the electron-transporting components (R_{ETC}). Dashed curves in Fig. 8*B* and *C* depict the resting terminal. Following stimulation, Ca^{2+} influx via the uniporter (I_{Ca} through R_{Ca}) is modelled by closing a switch, resulting in the continuous curves of Fig. 8*B* and *C* (see legend for further details).

When a large number of H^+-extruding complexes are available, the Ψ_m depolarization caused by Ca^{2+} influx into mitochondria drives a substantial increase in H^+ extrusion (open arrow in Fig. 8*C*) that limits the extent of Ψ_m depolarization (open arrow in Fig. 8*B*). Here, a reduction in the number of H^+-extruding complexes (e.g. by inhibiting complex I with amytal) has little effect on H^+ extrusion or Ψ_m in the resting terminal (dashed curves in Fig. 8*C* and *B*). But following stimulation, the increase in H^+ extrusion is smaller (solid arrow in Fig. 8*C*) and Ψ_m depolarization is greater (solid arrow in Fig. 8*B*).

In sum, measurements of changes in NADH fluorescence, Ψ_m and mitochondrial and cytosolic [Ca^{2+}] in motor nerve terminals suggest that the most immediate energy demand imposed by repetitive stimulation is associated with Ca^{2+} uptake into mitochondria, and that the Ψ_m depolarization produced by this Ca^{2+} influx drives increased H^+ extrusion via the ETC. This acceleration allows Ca^{2+} uptake to continue with minimal dissipation of Ψ_m. Strong reliance on mitochondria to buffer stimulation-induced Ca^{2+} loads may place motor terminals at risk during stresses and diseases associated with compromised ETC activity.

References

Angaut-Petit D, Benoit E & Mallart A (1989). Membrane currents in lizard motor nerve terminals and nodes of Ranvier. *Pflugers Arch* **415**, 81–87.

Billups B & Forsythe ID (2002). Presynaptic mitochondrial calcium sequestration influences transmission at mammalian central synapses. *J Neurosci* **22**, 5840–5847.

Bindokas VP & Miller RJ (1995). Excitotoxic degeneration is initiated at non-random sites in cultured rat cerebellar neurons. *J Neurosci* **15**, 6999–7011.

Blasi J, Chapman ER, Link E, Binz T, Yamasaki S, DeCamilli P, Sudhof TC, Niemann H & Jahn R (1993). Botulinum neurotoxin A selectively cleaves the synaptic protein SNAP-25. *Nature* **365**, 104–105.

Brandes R & Bers DM (1997). Intracellular Ca^{2+} increases the mitochondrial NADH concentraton during elevated work in intact cardiac muscle. *Circ Res* **80**, 82–87.

Brandes R & Bers DM (2002). Simultaneous measurements of mitochondrial NADH and Ca^{2+} during increased work in intact rat heart trabeculae. *Biophys J* **83**, 587–604.

Carafoli E (2003). Historical review: mitochondria and calcium: ups and downs of an unusual relationship. *Trends Biochem Sci* **28**, 175–181.

Chalmers S & Nicholls DG (2003). The relationship between free and total calcium concentrations in the matrix of liver and brain mitochondria. *J Biol Chem* **278**, 19062–19070.

Chinopoulos C, Tretter L & Adam-Vizi V (1999). Depolarization of in situ mitochondria due to hydrogen peroxide-induced oxidative stress in nerve terminals: inhibition of α-ketoglutarate dehydrogenase. *J Neurochem* **73**, 220–228.

Cochilla AJ, Angleson JK & Betz WJ (1999). Monitoring secretory membrane with FM-43 fluorescence. *Annu Rev Neurosci* **22**, 1–10.

Cunarro J & Weiner MW (1975). Mechanism of action of agents which uncouple oxidative phosphorylation: direct correlation between proton-carrying and respiratory-releasing properties using rat liver mitochondria. *Biochim Biophys Acta* **387**, 234–240.

Davey GP, Canevari L & Clark JB (1997). Threshold effects in synaptosomal and nonsynaptic mitochondria from hippocampal CA1 and paramedian neocortex brain regions. *J Neurochem* **69**, 2564–2570.

David G (1999). Mitochondrial clearance of cytosolic Ca^{2+} in stimulated lizard motor nerve terminals proceeds without progressive elevation of mitochondrial matrix [Ca^{2+}]. *J Neurosci* **19**, 7495–7506.

David G, Barrett JN & Barrett EF (1997). Stimulation-induced changes in [Ca^{2+}] in lizard motor nerve terminals. *J Physiol* **504**, 83–96.

David G, Barrett JN & Barrett EF (1998). Evidence that mitochondria buffer physiological Ca^{2+} loads in lizard motor nerve terminals. *J Physiol* **509**, 59–65.

David G, Talbot J & Barrett EF (2003). Quantitative estimate of mitochondrial [Ca^{2+}] in stimulated motor nerve terminals. *Cell Calcium* **33**, 197–206.

Degli-Esposti M (1998). Inhibitors of NADH-ubiquinone reductase: an overview. *Biochim Biophys Acta* **1364**, 222–235.

DiMauro S & Schon EA (2003). Mitochondrial respiratory-chain diseases. *N Engl J Med* **348**, 2656–2668.

Dodge FA Jr, Miledi R & Rahamimoff R (1969). Strontium and quantal release of transmitter at the neuromuscular junction. *J Physiol* **200**, 267–283.

Duchen MR (1992). Ca^{2+}-dependent changes in the mitochondrial energetics in single dissociated mouse sensory neurons. *Biochem J* **283**, 41–50.

García-Chacón L, Nguyen K, David G & Barrett EF (2006). Extrusion of Ca^{2+} from mouse motor terminal mitochondria via a Na^+/Ca^{2+} exchanger increases post-tetanic evoked release. *J Physiol* **574**, 663–675.

Gundersen CB, Katz B & Miledi R (1982). The antagonism between botulinum toxin and calcium in motor nerve terminals. *Proc R Soc Lond B Biol Sci* **216**, 369–376.

Gunter TE & Pfeiffer DR (1990). Mechanisms by which mitochondria transport calcium. *Am J Physiol Cell Physiol* **258**, C755–C786.

Hajnoczky G, Robb-Gaspers LD, Seitz MB & Thomas AP (1995). Decoding of cytosolic calcium oscillations in the mitochondria. *Cell* **82**, 415–424.

Hansford RG (1994). Physiological role of mitochondrial Ca^{2+} transport. *J Bioenerg Biomembr* **26**, 495–508.

Hayakawa Y, Nemoto T, Iino M & Kasai H (2005). Rapid Ca^{2+}-dependent increase in oxygen consumption by mitochondria in single mammalian central neurons. *Cell Calcium* **37**, 359–370.

Jo H, Noma A & Matsuoka S (2006). Calcium-mediated coupling between mitochondrial substrate dehydrogenation and cardiac workload in single guinea- pig ventricular myocytes. *J Mol Cell Cardiol* **40**, 394–404.

Kanki R, Nakamizo T, Yamashita H, Kihara T, Sawada H, Uemura K, Kawamata J, Shibasaki H, Akaike A & Shimohama S (2004). Effects of mitochondrial dysfunction on glutamate receptor-mediated neurotoxicity in cultured rat spinal motor neurons. *Brain Res* **1015**, 73–81.

Kann O, Schuchmann S, Buchheim K & Heinemann U (2003). Coupling of neuronal activity and mitochondrial metabolism as revealed by NAD(P)H fluorescence signals in organotypic hippocampal slice cultures of the rat. *Neuroscience* **119**, 87–100.

Kasischke KA, Viswasrao HD, Fisher PJ, Zipfel WR & Webb WW (2004). Neural activity triggers neuronal oxidative metabolism followed by astrocytic glycolysis. *Science* **305**, 99–103.

Kim MH, Korogod N, Schneggenburger R, Ho WK & Lee SH (2005). Interplay between Na^+/Ca^{2+} exchangers and mitochondria in Ca^{2+} clearance at the calyx of Held. *J Neurosci* **25**, 6057–6065.

Kirichok Y, Krapivinsky G & Clapham DE (2004). The mitochondrial calcium uniporter is a highly selective ion channel. *Nature* **427**, 360–364.

Kosterin P, Kim GH, Muschol M, Obaid AL & Salzberg BM (2005). Changes in FAD and NADH fluorescence in neurosecretory terminals are triggered by calcium entry and by ADP production. *J Membr Biol* **208**, 113–124.

Lardy HA, Johnson D & McMurray WC (1958). Antibiotics as tools for metabolic studies. I. A survey of toxic antibiotics in respiratory, phosphorylative and glycolytic systems. *Arch Biochem Biophys* **78**, 587–587.

Lemeshko VV (2002). Model of the outer membrane potential generation by the inner membrane of mitochondria. *Biophys J* **82**, 684–692.

Loew LM, Carrington W, Tuft RA & Fay FS (1994). Physiological cytosolic Ca^{2+} transients evoke concurrent mitochondrial depolarizations. *Proc Natl Acad Sci U S A* **91**, 12579–12583.

Lotscher HR, Winterhalter KH, Carafoli E & Richter C (1980). The energy-state of mitochondria during the transport of Ca^{2+}. *Eur J Biochem* **110**, 211–216.

Luciani DS, Misler S & Polonsky KS (2006). Ca^{2+} controls slow NAD(P)H oscillations in glucose-stimulated mouse pancreatic islets. *J Physiol* **572**, 379–392.

McCormack JG, Halestrap AP & Denton RM (1990). Role of calcium ions in regulation of mammalian intramitochondrial metabolism. *Physiol Rev* **70**, 391–425.

Magnus G & Keizer J (1997). Minimal model of β-cell mitochondrial Ca^{2+} handling. *Am J Physiol* **273**, C717–C733.

Matlib MA, Zhou Z, Knight S, Ahmed S, Choi KM, Krause-Bauer J, Phillips R, Altschuld R, Katsube Y, Sperelakis N & Bers DM (1998). Oxygen-bridged dinuclear ruthenium amine complex specifically inhibits Ca^{2+} uptake into mitochondria in vitro and in situ in single cardiac myocytes. *J Biol Chem* **273**, 10223–10231.

Mayevsky A & Rogatsky GG (2007). Mitochondrial function in vivo evaluated by NADH fluorescence: from animal models to human studies. *Am J Physiol Cell Physiol* in press.

Meiri U & Rahamimoff R (1971). Activation of transmitter release by strontium and calcium ions at the neuromuscular junction. *J Physiol* **215**, 709–726.

Mironov SL & Richter DW (2001). Oscillations and hypoxic changes of mitochondrial variables in neurons of the brainstem respiratory centre of mice. *J Physiol* **555**, 227–236.

Morita K & Barrett EF (1989). Calcium-dependent depolarizing potentials originating in lizard motor nerve terminals. *J Neurosci* **9**, 3359–3369.

Mozhayeva MG, Matos MF, Liu X & Kavalali ET (2004). Minimum essential factors required for vesicle mobilization at hippocampal synapses. *J Neurosci* **24**, 1680–1688.

Narita K, Akita T, Osanai M, Shirasaki T, Kijima H & Kuba K (1998). A Ca^{2+}-induced Ca^{2+} release mechanism involved in asynchronous exocytosis at frog motor nerve terminals. *J Gen Physiol* **112**, 593–609.

Nicholls DG (1974). The influence of respiration and ATP hydrolysis on the proton-electrochemical gradient across the inner membrane of rat-liver mitochondria as determined by ion distribution. *Eur J Biochem* **50**, 305–315.

Nicholls DG (2005). Mitochondria and calcium signaling. *Cell Calcium* **38**, 311–317.

Nicholls DG & Ward MW (2000). Mitochondrial membrane potential and neuronal glutamate excitotoxicity: mortality and millivolts. *Trends Neurosci* **23**, 166–174.

Pralong WF, Spat A & Wollheim CB (1994). Dynamic pacing of cell metabolism by intracellular Ca^{2+} transients. *J Biol Chem* **269**, 27310–27314.

Robb-Gaspers LD, Burnett P, Rutter GA, Denton RM, Rizzuto R & Thomas AP (1998). Integrating cytosolic calcium signals into mitochondrial metabolic responses. *EMBO J* **17**, 4987–5000.

Rodriguez-Estrada C (1975). Reduced nicotinamide adenine dinucleotide and depolarization in neurons. *Am J Physiol* **228**, 996–1001.

Rohacs T, Nagy G & Spat A (1997). Cytoplasmic Ca^{2+} signalling and reduction of mitochondrial pyridine nucleotides in adrenal glomerulosa cells in response to K^+, angiotensin II and vasopressin. *Biochem J* **322**, 785–792.

Sadek HA, Szweda PA & Szweda LI (2004). Modulation of mitochondrial complex I activity by reversible Ca^{2+} and NADH mediated superoxide anion dependent inhibition. *Biochem* **43**, 8494–8502.

Schuchmann S, Kovacs R, Kann O, Heinemann U & Buchheim K (2001). Monitoring NAD(P)H autofluorescence to assess mitochondrial metabolic functions in rat hippocampal-entorhinal cortex slices. *Brain Res Brain Res Protoc* **7**, 267–276.

Schuchmann S, Luckermann M, Kulik A, Heinemann U & Ballanyi K (2000). Ca^{2+}- and metabolism-related changes of mitochondrial potential in voltage-clamped CA1 pyramidal neurons in situ. *J Neurophysiol* **83**, 1710–1721.

Shuttleworth CW, Brennan AM & Connor JA (2003). NAD(P)H fluorescence imaging of postsynaptic neuronal activation in murine hippocampal slices. *J Neurosci* **23**, 3196–3208.

Sørensen JB (2004). Formation, stabilisation and fusion of the readily releasable pool of secretory vesicles. *Pflugers Arch* **448**, 347–362.

Suzuki S, Osanai M, Mitsumoto N, Akita T, Narita K, Kijima H & Kuba K (2002). Ca^{2+}-dependent Ca^{2+} clearance via mitochondrial uptake and plasmalemmal extrusion in frog motor nerve terminals. *J Neurophysiol* **87**, 1816–1823.

Talbot JD, David G & Barrett EF (2003). Inhibition of mitochondrial Ca^{2+} uptake affects phasic release from motor terminals differently depending on external Ca^{2+}. *J Neurophysiol* **90**, 491–502.

Van Buuren KJH, Zuurendonk PF, Van Gelder BF & Muijsers AO (1972). Biochemical and biophysical studies on cytochrome aa_3. V. Binding of cyanide to cytochrome aa_3. *Biochim Biophys Acta* **256**, 243–257.

Vergun O & Reynolds IJ (2005). Distinct characteristics of Ca^{2+}-induced depolarization of isolated brain and liver mitochondria. *Biochim Biophys Acta* **1709**, 127–137.

Voronina S, Sukhomlin T, Johnson PR, Erdemli G, Petersen OH & Tepikin A (2002). Correlation of NADH and Ca^{2+} signals in mouse pancreatic acinar cells. *J Physiol* **539**, 41–52.

Votyakova TV & Reynolds IJ (2005). Ca^{2+}-induced permeabilization promotes free radical release from rat brain mitochondria with partially inhibited complex I. *J Neurochem* **93**, 526–537.

Wakamori M, Strobeck M, Niidome T, Teramoto T, Imoto K & Mori Y (1998). Functional characterization of ion permeation pathway in the N-type Ca^{2+} channel. *J Neurophysiol* **79**, 622–634.

Warashina A (2006). Mode of mitochondrial Ca^{2+} clearance and its influence on secretory responses in stimulated chromaffin cells. *Cell Calcium* **39**, 35–46.

Ward MW, Rego AC, Frenguelli BG & Nicholls DG (2000). Mitochondrial membrane potential and glutamate excitotoxicity in cultured cerebellar granule cells. *J Neurosci* **20**, 7208–7219.

Acknowledgements

This work was supported by NIH grants NS 12404, NS 49374 and NS 12207, grants 0455215B and 0555150B from the Florida Affiliate of the American Heart Association, and by the Muscular Dystrophy Association. J.T. was supported by 2T32 NS 07044 during a portion of this work. Purchase of the confocal microscope was enabled by NIH shared equipment grant 1S10 RR16856.